ORIGINAL PAPER

Tsunami evacuation simulation considering road blockage by collapsed buildings evaluated from predicted strong ground motion

Eri Ito[1] · Hiroshi Kawase[1] · Shinichi Matsushima[1] · Michinori Hatayama[1]

Abstract

Tsunami evacuation simulations are often used to determine necessary countermeasures that will reduce human loss effectively after earthquakes and subsequent tsunamis. However, so far there has been no simulation for the estimated building damage using up-to-date knowledge of seismic engineering. In this study, in order to clarify the effect of building damage on a tsunami evacuation, we first predicted building damage based on the nonlinear response analysis for a realistic strong ground motion and then simulated a tsunami evacuation considering road blockage due to the collapsed buildings. We used one district in Tanabe City in Wakayama Prefecture in Japan where we expect to have a 12 m of tsunami height after an earthquake along the Nankai Trough plate boundary. We found that the prepared capacity of evacuation sites is not enough to let everyone evacuate and that the number of survivors increases by 3–4% if all of the buildings and houses are seismically reinforced. Considering this, plus 1% of expected casualties inside the collapsed houses, it appears to be not as efficient to reinforce buildings and houses to prevent human loss in comparison with increasing the capacity of tsunami evacuation sites in the target district. However, the damage to building and houses will cause a lot of side effects which are not considered here, but will prolong the evacuation time. Thus, we concluded that we need to reinforce the buildings and houses as well as consider the appropriate placement, number, and capacity of the evacuation sites.

✉ Eri Ito
  ito@sere.kyoto-u.ac.jp

  Hiroshi Kawase
  kawase@sere.dpri.kyoto-u.ac.jp

  Shinichi Matsushima
  matsushima@sds.dpri.kyoto-u.ac.jp

  Michinori Hatayama
  hatayama@imdr.dpri.kyoto-u.ac.jp

[1] Disaster Prevention Research Institute, Kyoto University, Gokasho, Uji-shi, Kyoto, Japan

1 Introduction

Given the imminent occurrence of an earthquake or earthquakes along the Nankai Trough plate boundary, developing effective countermeasures has become an urgent priority on the southwestern side of Japan. However, the finances of local governments are constrained, making this a difficult goal to achieve. At the same time, local residents are of an older age and often lack a concrete understanding of the looming disaster or else they feel a sense of defeat about it. (That is to say, they are driven to despair.) To keep motivation within residents inside the tsunami inundation areas for tsunami evacuation activities immediately after the large mega-thrust earthquake, we need to interact with them through dissemination of information and discussion on what will happen when the mega-thrust earthquake occurs offshore of their city or town and stimulate their imagination through a concrete picture of tsunami disaster scenarios that should be expected based on scientifically rational (i.e., evidence-based) simulations (e.g., Nakai et al. 2014).

As far as we have surveyed, one of the first papers related to tsunami evacuation simulation using agents seems to be Usuzawa et al. (1997). They performed the tsunami evacuation simulation in the area damaged by the 1993 Hokkaido–Nansei–Oki earthquake for future evacuation planning, and they showed that the result was validated by the detailed surveys just after the earthquake. Since then, many papers have been published, mainly focusing on the parameters used in the simulation in order to make them more realistic. For instance, the interaction between pedestrians and motorcycles or cars has been considered (Goto et al. 2012; Mas et al. 2012, 2013; Makinoshima et al. 2016). Among them, Goto et al. (2012) assumed that the walking speed as well as the motorcycle speed decreased with increased density and then simulated the cases with different ratios between pedestrians and motorcycles. They also presented the simulation to the elementary, middle, and high school students in the target area as a course of disaster education and proved that their simulations made easy for students to understand the appropriate evacuation procedure. Mas et al. (2012) introduced a new approach to model the starting time of evacuation based on the sigmoid curve, as they thought that the starting time may have a significant effect on congestions and bottlenecks during evacuation. Thus, progress of tsunami evacuation simulation has been made and these simulations provide various tools for the evacuation planning. Based on such progress, Hori et al. (2015) considered that there remains uncertainty in these tsunami evacuation simulations and suggested a way to evaluate the quality of the simulation.

As for the effects of building damage on evacuation routes, we found only a few reports of the tsunami simulation considering building collapse and subsequent road blockage. For example, Sato et al. (2002) adopted the vulnerability function developed by Murao (1999) for the damage estimate. Tamura et al. (2005) adopted a probability distribution model that predicts the width of the debris depending on the JMA seismic intensity estimated by Akakura et al. (2000). Later Sakata and Teraki (2009) predicted in their tsunami evacuation simulations which buildings would collapse by surveying their ages or observing building exteriors. They proposed a model that can vary the rubble flow distance based on the probabilistic distribution of collapsed directions (i.e., randomly distributed to all directions).

In these pioneering studies, their focus was not primarily on the quantification of expected building damage. The structural damage that buildings are likely to incur depends on a complex combination of multiple factors, including the building's vibration characteristics, seismic input motion characteristics, and the softness of the surrounding ground. Damages should therefore be quantitatively estimated using an up-to-date technology in

earthquake engineering. Since traditional methods have not considered the seismic motion characteristic and the ground characteristics, it is likely that the real outcome will differ from the simulation results. In contrast to the Great East Japan Earthquake of 2011, in which building damages were relatively small (e.g., Baoyintu et al. 2013), there is a concern that building damages caused by seismic motion will be greater for an earthquake along the Nankai Trough, due to the fact that the hypocentral region will be closer to the shore (e.g., Central Disaster Prevention Council 2003; Ho and Kawase 2008). Road blockages caused by collapsed buildings are expected to pose a greater obstacle for residents trying to evacuate before the tsunami hits.

If the estimates of building damages used in an evacuation simulation undertaken for the purpose of disaster impact analysis and subsequent development of countermeasures for disaster reduction deviates greatly from the actual outcome, countermeasures based on that inaccurate estimate may not be quite effective. In order to avoid this, the tsunami evacuation simulations undertaken in the present study predicted building damage by incorporating three major factors—the buildings themselves, ground characteristics, and input ground motions—using the knowledge available in earthquake engineering.

Strong ground motion simulations based on the physics-based methodology with a scenario-type representation of the source process have been getting popular in recent years, as evidenced by the institutional activities in Japan as well as in the USA (National Research Institute for Earth Science and Disaster Resilience 2013; Southern California Earthquake Center 2018). As for the Nankai Trough mega-thrust earthquakes, the Central Disaster Prevention Council released multiple scenarios with different source sizes and rupture patterns, where structural damages as well as human losses are estimated based on both strong ground motions and tsunami inundation heights (Central Disaster Prevention Council 2003, 2011). The most recent rupture scenario of the Nankai Trough earthquakes by the Central Disaster Prevention Council is a magnitude 9.1 four-segment-rupture scenario in which an extraordinarily large length, width, and slip amount are assumed (Central Disaster Prevention Council 2012). The probability of occurrence for such an extraordinary source scenario should be close to null. More plausible scenarios based on the source parameters for the earthquakes in the past are used by several researchers in their quantitative strong motion simulations (e.g., Kamae and Irikura 1994; Ho and Kawase 2008; Baoyintu 2014), whose ground motions are reasonably smaller than those by Central Disaster Prevention Council (2012).

Structural damage predictions should also be physics-based in order to fully utilize the characteristics of the simulated ground motions. This means that we need to construct structural response models used for structural damage predictions. In the current practice of structural damage predictions, we usually use a vulnerability function of a specific level of damage such as total damage, half damage, and partial damage, obtained empirically from the damage statistics of previous earthquakes (e.g., Murao and Yamazaki 2002). The largest problem with this vulnerability function approach is the ignorance of the effects of the difference in ground motion characteristics for crustal earthquakes and subduction zone earthquakes. The current empirical vulnerability functions in Japan are primarily determined by the damage statistics from the 1995 Hyogo-ken Nanbu (Kobe) earthquake and therefore should not be used for the damage prediction of the Nankai Trough plate boundary earthquakes. As described later, we use structural response analysis of multi-degree-of-freedom models specific to different types of buildings and different construction years (Nagato and Kawase 2001, 2002a, b).

This study simulated tsunami evacuations in which we considered that collapsed wooden houses would block escape routes in order to evaluate the effectiveness of the

current evacuation sites in terms of their locations and capacities. It aimed to quantitatively demonstrate the effects of earthquake-resistant reinforcements on evacuation speed, and thus provide vital information for selecting the most effective countermeasures for mega-thrust earthquakes along the Nankai Trough plate boundary.

2 The target district for this study

For this study, we chose a district comprising 1-, 2-, and 3-Chome of Kamiyashiki and a part of Katamachi, located along the coastline of Tanabe City, Wakayama Prefecture. The district is shown in Fig. 1 (red area). The population is approximately 1250 people in 641 households (Tanabe City 2013a). The predicted maximum JMA seismic intensity in the district is 7, in the event of a simultaneous rupture with three consecutive segments, with a 12 m tsunami estimated to arrive approximately 15 min at earliest after the earthquake. Here, JMA seismic intensity is the one determined by the Japanese Meteorological Agency which is an index to categorize the intensity of local ground shaking into 10 categories (but 7 is the highest) indicated by the logarithm of peak ground acceleration. Please refer to Karim and Yamazaki (2002) on how to calculate JMA intensity.

Figure 2 shows the final inundation area around the target district (Tanabe City 2014). On the map, the Nippon Telegraph and Telephone Corporation (NTT) building and the Tanabe Daiichi Primary School (hereafter "the Primary School") are the designated tsunami evacuation buildings, and Tokei Shrine, which is next to a small hill with the capacity for all the people in the target district, has also been designated as an evacuation area. (These tsunami evacuation buildings and the evacuation area are shown as black stars in Figs. 1, 2.) Hereafter, we refer to this evacuation site of a small hill behind Tokei Shrine simply as "Tokei Shrine." However, Tokei Shrine is at least 620 m away from Kamiyashiki, meaning that it would take residents 14–15 min to reach the shrine on foot and is too far away for elderly persons. The district also has many traditional wooden houses remaining.
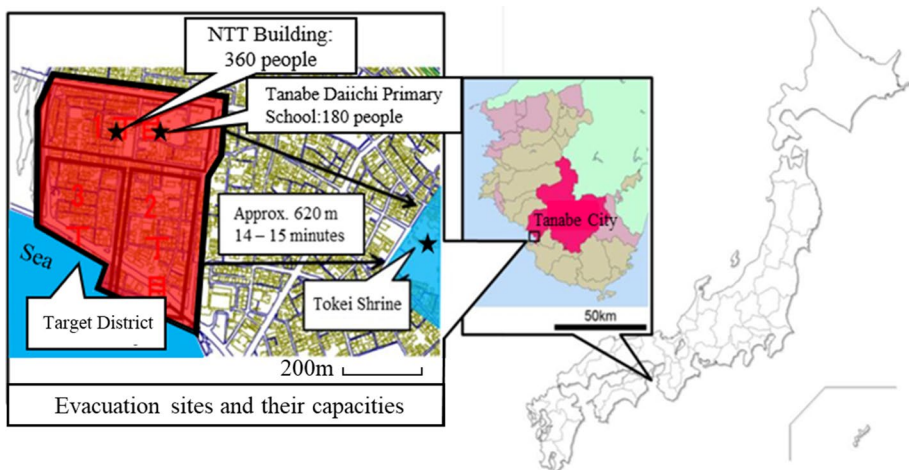

Fig. 1 Target district for this study, in the southwestern side of Tanabe City, Wakayama Prefecture, Japan. Two evacuation sites, namely the NTT Building and the Tanabe Daiichi Primary School, inside of the target district and one evacuation site outside, Tokei Shrine, are shown by star symbols
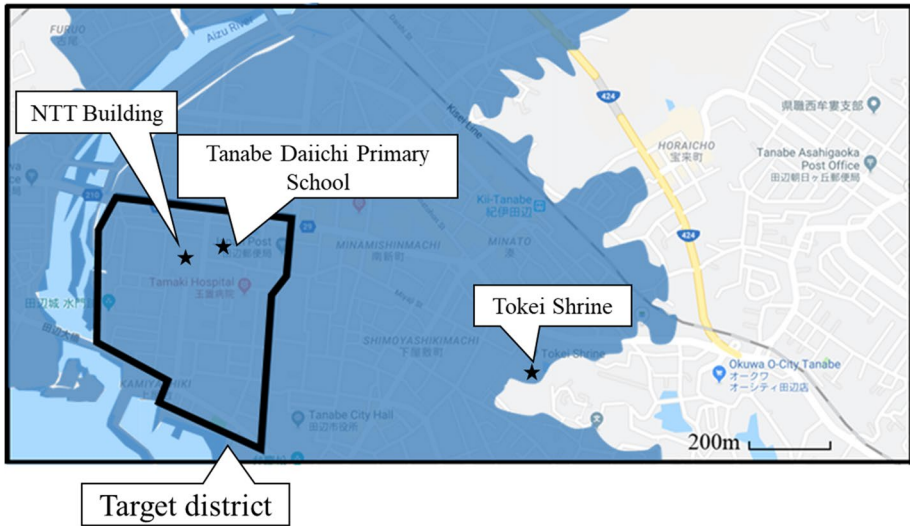
Fig. 2 A map of the expected inundation area of tsunami around the target district (Tanabe City 2014)

In the event of an earthquake, it is important to escape from houses and start to evacuate as soon as possible in order to avoid the tsunami that follows. For this, however, it is a prerequisite that houses will maintain their integrity and safety after the earthquake. When we asked a city official of Tanabe City about the awareness of the residents to the earthquake, he told us that many of them did not realize that safe evacuation might be delayed or rendered impossible if non-earthquake-resistant houses were heavily damaged during an earthquake.

Tanabe City developed and published an earthquake resistance countermeasure plan based on predictions of heavy building damage during a Nankai Trough earthquake. The old plan aimed to halve the number of non-earthquake-resistant houses between 2006 and 2015, raising the proportion of earthquake-resistant houses from 56% in 2005 to 80% by 2015. The current plan aims to raise the proportion of earthquake-resistant houses from 75% as of the end of 2015 to 95% by the end of 2020 (Tanabe City 2016). The city committed to providing free earthquake resistance diagnoses and partial financial assistance for seismic reinforcement design and retrofitting implementation for those houses that scored less than 1.0 in the diagnosis, as well as commissioning workers to affix furniture for elderly and handicapped residents. However, according to Tanabe City, the number of buildings that can be made earthquake-resistant annually is only approximately 1% of all the non-earthquake-resistant buildings. At this rate, it would be difficult to meet the goals within the allocated time frame.

3 Predicting building collapse

As mentioned in "Introduction," building damage predictions have usually been made using a "vulnerability function approach," which depends on an empirically identified correlation between the strength index of the observed ground motion such as the peak ground acceleration or the seismic intensity and the damage level around the

observation point, that is, the ratio of numbers of heavily damaged or collapsed buildings to those of the total buildings inside the designated area. However, it is difficult to observe ground motions at locations where damage ratios are high because strong motion observation sites are still sparse, and therefore, it is difficult to measure accurate vulnerability functions in locations with severely damaged structures, where they are of utmost importance. It is also difficult to determine the most appropriate size of the areas used for evaluating damage ratios. Furthermore, vulnerability functions are calculated with respect to one of the strength indices of ground motion, which could not fully represent the structural impact of ground motions from different types of sources, namely crustal earthquakes and subduction zone earthquakes. Taking these limitations into consideration, Nagato and Kawase (2001, 2002a, b) developed a new damage prediction method founded on nonlinear response analysis of buildings that does not depend on such preconditions, and demonstrated that the model was sufficiently practicable. They reported that the model successfully approximated actual recorded damages during the 2005 West off Fukuoka earthquake (Kawase 2007) and the 2011 Tohoku earthquake (Baoyintu et al. 2013). The latter is important to the present study, as the Tohoku earthquake had a long duration of motion, similar to what is expected during the Nankai Trough mega-thrust earthquakes. Their prediction methodology is briefly described below. (Please refer to the cited articles for further details.)

Nagato and Kawase's model (Nagato and Kawase 2001, 2002a, b) was constructed through the following procedure.

First, a story-wise multiple shear spring–mass model with nonlinear behavior was constructed as a single-column model. Next, multiple models of which the yield strength varies in the specific building category were prepared for different building types and number of floors, and their existence ratios were estimated based on the log-normal distribution from the investigation of numbers of buildings in the past. Their existence ratio distribution with respect to yield strength is important to reproduce the observed damage ratio at the target point from a single-input motion there.

Reproduced strong motions (Matsushima and Kawase 2000) were applied to the models at every 60 m by 120 m grids, and the damage ratio was calculated as the sum of the ratio of the models that suffered major damage according to given criteria. Then the average yield strength was estimated in order to reproduce the average of the observed building damage ratio in the Nada-Ku and Higashinada-Ku districts during the Hyogo-ken Nanbu (Kobe) earthquake of 1995. Please note that the damage ratio here was the one surveyed by the structural experts of Architectural Institute of Japan based on Rank 4 and Rank 5 shown in Okada and Takai (2004), which corresponds to the damage level as "severely damaged" (Rank 4) or "collapsed" (Rank 5). The following conditions were assumed for reinforced concrete (RC) and steel construction:

1. The shape of the yield strength distribution (the average of the distribution was estimated through calculation) is log-normal with a fixed standard deviation.
2. Destruction criteria (any floor exceeding the threshold was deemed heavily damaged or collapsed) are assumed based on laboratory experiments.
3. The vertical shear stiffness distribution was given by the "A_i" distribution in the current building code. The value "A_i" is the coefficient of the shear force coefficient with respect to the base shear coefficient as a function of the floor height, which reflects the vertical distribution of the shear force coefficient in each floor for design.
4. Any soil–structure interaction was ignored due to cancelation with soil amplification.

These assumptions were different for wooden houses in 1) and 3), where the detailed statistics of actual wooden houses in Kobe were used.

In order to accurately reproduce the effect of the natural period of the building on the response, four models were created for RC structure (3-, 6-, 9-, and 12-storied buildings for both buildings with older earthquake resistance standards, and those with new standards after the large code modification in 1981), and three models were created for steel construction (3, 4, and 5 stories, also divided into old and new standards). For wooden construction, only a two-storied model with no age differentiation was used, as this model was representative of the majority of wooden construction houses in the target district. A group of models was thus created based on these assumptions. Matsushima and Kawase's reproduced strong ground motions (Matsushima and Kawase 2000) were input into the models, and damage ratios were computed and compared to the observed damage ratios. By repeatedly changing the average yield strength, each model's ability to accurately reproduce the damage ratios was attained.

Figure 3 shows the ratio of the optimized yield strength for each building category to the yield strength of the standard building (corresponding to the yield strength as the minimum requirement of the design code in 1981). For the two-storied wooden building with no age differentiation, this ratio was 1.95. The yield strengths thus obtained for the group of building models were considerably larger than those of standard building models in the case of wooden and low-storied RC constructions. Nagato and Kawase (2001, 2002a, b) attributed this to the contribution of non-structural elements of buildings to their yield strengths. On
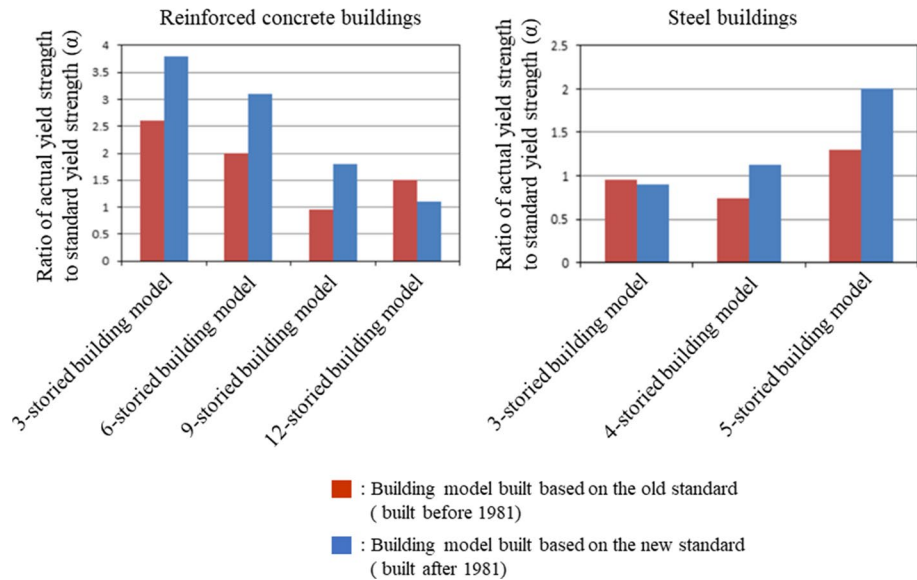

Fig. 3 Ratios of the actual yield strength to the standard (code required) yield strength for models that can reproduce observed damage ratios in Kobe during the 1995 Hyogo-ken Nanbu (Kobe) earthquake for reinforced concrete buildings (left) and steel buildings (right). Apparent differences in the yield strengths can be seen between buildings built before and after 1981 when a large code modification took place, except for 12-storied RC building models and three-storied steel building models. After Nagato and Kawase (2001, 2002a, b)

the other hand, the yield strengths for low-storied steel construction buildings were almost the same as those of the standard building models, and it could be said for steel construction buildings to be comparatively more vulnerable.

The validity of the building models has been confirmed as follows: When the reproduced seismic wave was applied, the maximum inter-story drift angle distribution matched well with those observed during the Hyogo-ken Nanbu (Kobe) earthquake of 1995, and the calculated damage ratio distribution matched the observed distribution in the Nada-ku and Higashinada-Ku districts of Kobe City.

In the present study, the time history wave of the ground motion predicted for the target district in the event of a consecutive rupture scenario for three Nankai–Tonankai–Tokai segments (Baoyintu 2014) of M8.7 was applied to the building models, and the damage ratios were computed. The amplification factor for the surface subsoil in the target district was generally homogenous [between 1.4 and 1.6 according to J-SHIS amplification factor (National Research Institute for Earth Science and Disaster Resilience 2013)]; therefore, the seismic wave was not corrected for the effect of surface subsoil at different ground points. In districts where there is considerable spatial variation in the shallow subsoil structure, amplitude corrections must be made based on an index for the spatial variation in the shallow subsoil structure such as Vs30, an average S-wave velocity from the surface to a depth of 30 meters.

The diagrams here show the amplification factor for the target district (Fig. 4) based on the J-SHIS (National Research Institute for Earth Science and Disaster Resilience 2013) and the damage ratios obtained by applying the predicted input waves (Fig. 5). Note that the "damage ratio" here is the percentage of buildings that suffered heavy damage or collapsed.

4 Tsunami evacuation simulation using agent methodology

4.1 Summary of the tsunami evacuation evaluation system

An agent-based simulator (hereafter "simulator") was used for tsunami evacuations, and the space–time geographic information system (hereafter "space–time GIS") was structured in such a way as to share the same database. The former was constructed on a multi-agent platform "Aritsoc" (Kaneda 2010) developed and distributed by Kozo Keikaku Engineering Inc., and the latter was built on "DiMSIS" (Hatayama 1999), a space–time GIS system developed by Disaster Prevention Research Institute, Kyoto University. The only agents in this platform are people, and the underlying data are provided from a database. The data comprise the basic attributes of the residents, information collected from site surveys, and the geographic characteristics of the target district. The geographic characteristics, based on publicly available data, are organized on the space–time GIS system and stored in the database.

The position and direction of motion of the agents at each simulation step are incorporated into the space–time GIS system and overlaid with the tsunami inundation simulation. The movements of the agents are then collated and evaluated, and finally visualized as space–time data. In our study, the residents' basic attributes were configured as follows:

1. Initial positions of agents: nighttime was assumed, and agents were initialized inside their homes. Agents were generated based on a register containing population and
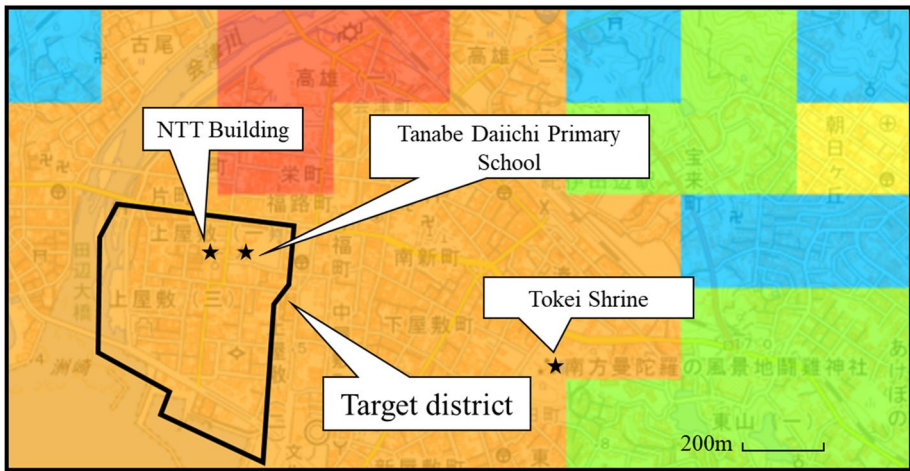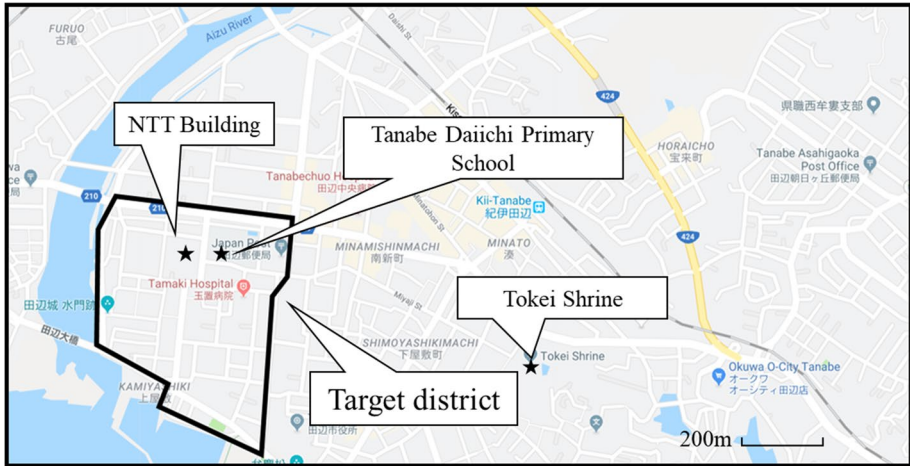
Fig. 4 Soil amplification factor in the target district (National Research Institute for Earth Science and Disaster Resilience 2013; Baoyintu 2014)

Fig. 5 Predicted damage ratios for different building types (*w* wooden houses, *RC* reinforced concrete, *S* steel), number of stories, and old/new standards using the damage prediction code (Nagato and Kawase 2001, 2002a, b). No difference for construction years is considered in wooden houses
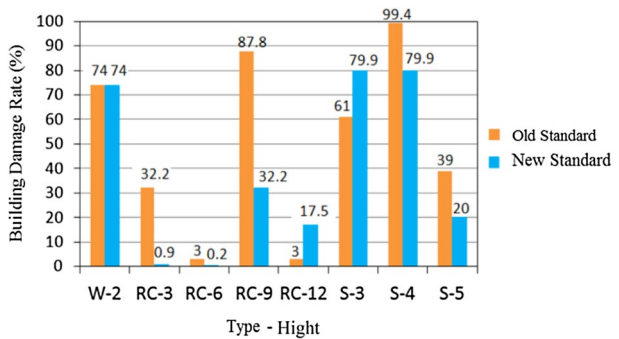
household data by town (Tanabe City 2012) and the population records by town and age (Tanabe City 2013b) published on Tanabe City's Web site. The resident register is broken down by block, gender, and age in five-year increments. Using this information, average households and family members were constructed and randomly distributed among buildings in the target district.

2. Evacuation speeds: based on interviews the Ministry of Land, Infrastructure and Transport conducted with tsunami evacuees of the 2011 Great East Japan Disaster (Ministry of Land, Infrastructure, Transport and Tourism 2012), an average walking speed of 2.65 km per hour was assumed for residents between 10 and 69 years of age, and 1.88 km per hour for residents younger than 10 or older than 70, and 1.96 km per hour in case that residents between 10 and 69 years are evacuating with children under 10 or elderly people over 70.

3. Time required to start evacuation: we allowed for 3 min during the earthquake when residents cannot move (2 min for shaking to settle and 1 min to prepare for evacuation) and added 2 min as best effort required, totaling 5 min. The 5 min for best effort was set by taking into consideration the testimonies regarding the time required to commence evacuation from survivors of the Great East Japan Disaster (Geospatial Information Authority of Japan 2013). The starting point of evacuation was assumed to be the road in front of each house.

4. Initial direction: the initial direction was set as the direction of the first destination node, which was dependent on the location of the evacuee's house.

5. Method of transportation: for the purpose of this study, we assumed that no cars would be used and all evacuees would be moving on foot.

The main purpose of this study is not to evaluate the effects of each parameter assumed in the simulation, but to evaluate the effects of damaged buildings and the arrangement of evacuation sites. For that purpose, each parameter above is the most plausible one where we consider the simplest case, that is, the case when the residents are trained enough to start evacuation immediately after the earthquake, and they fully understand the risk of using cars for their evacuation.

4.2 Geographic space information

The 1:2500 scale fundamental geospatial data provided by the Geographical Survey Institute (Ministry of Land, Infrastructure, Transport and Tourism 2011) were used as the base map. The resolution of the map is 5 m in both horizontal and vertical directions. In order to generate evacuation routes, "road curbs" and "buildings" corresponding to residential areas were extracted from the map, and the remaining information was used as the background of the presentation map. Evacuation routes can be divided into intersections and the segments that connect the intersections ("movement path section"), along which agents can move. The curbs at both sides of the routes were marked with dots in approximately every 50 cm increments to digitally enclose the path. Representative nodes at each intersection were assigned node numbers (Fig. 6).

For the movement path segments, first we divided the segment into small triangles and then a representing point was placed near one side of the triangle. Its attribute was assigned so that agents would allow movement toward the next intersection, that is to say, the movement in the forward direction along the path. "Forward direction" here refers to the direction from one intersection to the next, from the smaller node number to a larger node
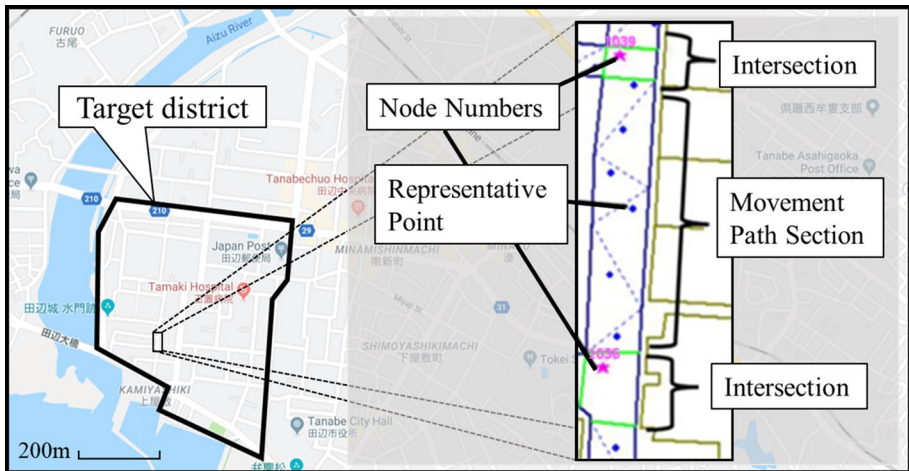
Fig. 6 An example of the evacuation path in DiMSIS, the space–time GIS used for simulation. The movement path section is defined as the path between two intersections with node numbers, and it is divided into small triangles in which one representative point is placed to give an attribute for forward and backward directions of motion

number. Data were prepared so that by specifying the final destination node at each starting node (i.e., for evacuees starting from that node), the data would show the next node toward which each evacuee should head. These routes were determined by a shortest path finding algorithm (Nakai and Hatayama 2013a, b). Simulation results (Suzuki et al. 2011) for an M8.7 consecutive rupture scenario for three Nankai–Tonankai–Tokai segments following the assumptions made by the Central Disaster Prevention Council (Central Disaster Prevention Council 2011) were used to simulate tsunami motion. Figure 7 illustrates the example of the tsunami evacuation simulation at one lapse time, 23 min after the earthquake.

5 Summary of the tsunami evacuation simulation

After preparing the prerequisite information as outlined in Sect. 4 and taking into consideration the building damage ratios predicted in Sect. 3, a tsunami evacuation simulation was performed. Parameters used for the simulation were as follows: tsunami data, number and initial positions of residents, position and capacity of evacuation sites, walking speed, and number and locations of collapsed buildings. The simulation outcome averaged three trials for each of the 210 patterns, comprising the combination of two patterns of the evacuation sites described below and fifteen road blockage patterns, each with a proportion of earthquake-resistant buildings assumed at 0%, 10%, 30%, 50%, 70%, 90%, and 100%. In each of the three trials, routes of individual agents to the evacuation sites were varied, because we selected priority of evacuees by different random numbers at each path at each time and the different selection will be made whenever the number of evacuees exceeded the path capacity. However, in all 210 simulations, variations of the number of the successful evacuees between three trials were small. This may be so because the occurrence of the exceeding path capacity was not so frequent. The parameters for the tsunami evacuation simulation are described in detail below.
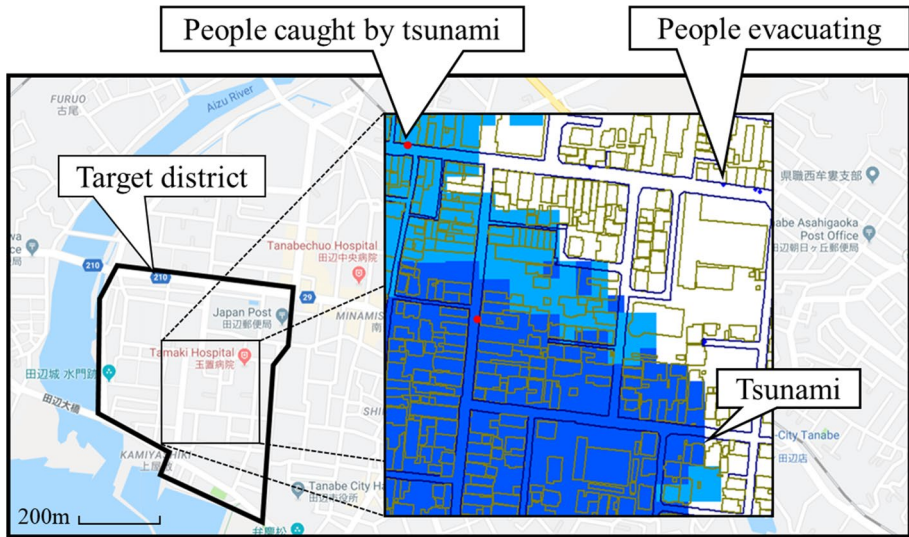
Fig. 7 A tsunami evacuation simulation example. Dots on the streets represent evacuees

5.1 Patterns for evacuation sites

The first simulation was performed assuming that both residents in Kamiyashiki 3-Chome, which is situated furthest from the elevated ground and therefore deemed most difficult to evacuate, and residents in the southern part of Kamiyashiki 2-Chome, which the tsunami will hit first, would evacuate to the NTT building and the Primary School. Remaining residents would evacuate to Tokei Shrine. This simulation was designed to help determine whether the capacity, number, and locations of the evacuation sites would be sufficient. The evacuation plan was deemed the most ideal according to the current circumstances, and it is referred to as Case 1.

Next, another scenario, in which everyone was evacuated to Tokei Shrine, was simulated to determine the effectiveness of the capacity and position of the evacuation buildings, namely the NTT building and the Primary School used in Case 1. This is referred to as Case 2.

5.2 Road blockages caused by collapsed buildings

In the simulations, the number of collapsed buildings was calculated using the building damage simulation program introduced in Chapter 3, together with the approximated ratio of 4:3, which is the number of buildings that were severely damaged versus the number of buildings that collapsed or disintegrated, as per the investigation report by the Architecture and Earthquake Investigation Committee for Chuo-Ku, Kobe City (Central Disaster Prevention Council 2003). Since buildings suffered from severe damage (Rank 4 level in Okada and Takai (2004) criteria) can still stand upright after the earthquake, we should exclude them in the road blockage estimation. The schemes for determining the buildings that would collapse and for generating the patterns of road blockages are described below.

Fig. 8 Locations of non-wooden buildings and wooden houses in the district. Although the construction age, built before and after 1981, in both non-wooden buildings and wooden houses is distinguished in the database, the latter is not referred to in this study

Table 1 Numbers of collapsed buildings for different construction types estimated by Nagato and Kawase's model (2001, 2002a, b)

Construction	(a) Total	(b) Damage rate (%)	(c) Collapse rate (%)	(d) Number of collapsed buildings = (a) × (c) × 1/100
Wooden	257	74.0		82
Non-wooden (RC, old standard)	11	32.2		1
Non-wooden (RC, new standard)	12	0.9	(b) × 3/7	0
Non-wooden (S, old standard)	27	61.0		7
Non-wooden (S, new standard)	56	79.9		19
Unknown construction	268	70.9		81

1. Buildings that could be determined to be wooden or non-wooden construction using Google Earth and onsite surveys were categorized accordingly and then numbered. Wooden construction buildings were numbered from 1 to 257, and non-wooden buildings were numbered from 1 to 106. Buildings for which construction could not be determined were numbered from 1 to 268 (Fig. 8).

2. For the collapsed buildings, the number of each type of building was multiplied by the damage ratio from Nagato and Kawase's simulation program in order to determine the number of buildings that would suffer major damages or collapse. This number was then multiplied by 3/7, which is the estimated proportion of buildings that would collapse among buildings that suffered major damages and higher, in order to compute the total number of collapsed buildings. Table 1 shows these numbers. Note that (a) the number of each type of non-wooden construction buildings (i.e., RC or steel) was computed by multiplying the ratio of the respective building type as recorded on the Tanabe City

taxation roll (Tanabe City 2008) by the total number of buildings, 106; and (b) the damage ratios shown in Fig. 5 were used to calculate damages to wooden and non-wooden construction buildings. For buildings of unknown construction type, the total damage ratio of 70.94% was used. This ratio was derived by multiplying Nagato and Kawase's damage ratio by the building group model and adding the results together.

3. The buildings that collapsed were selected using a random number generator across the number of buildings of each construction type (wooden, non-wooden, and unknown), as the one building collapse pattern. By doing the same process 14 times, we got the 15 building collapse patterns. The buildings that collapsed at each level of earthquake resistance were also chosen by randomly selecting assigned numbers.

4. After the shapes of the buildings chosen in step 3) were determined using DiMSIS, road blockages were created. Three levels of road blockage were assumed based on the road width as follows:

   (a) Roads with the widths less than 3 m: complete blockage if one of the houses on either side of the road collapsed.
   (b) Roads with widths greater than 3 m, but less than 6 m: roads were not completely blocked if a house on the one side of the road collapsed, but were blocked completely if two opposing houses collapsed.
   (c) Roads with widths greater than 6 m: no effect on passage even if houses on both sides of the road collapsed.

The above standard was based on a rubble flow distance of 3 m. Since we were unable to find a quantitative source for rubble flow distance, it was assumed to be 3 m when the first floor of a two-storied building, which is the most typical in the target district for this study, collapsed. Furthermore, the direction of the flow was assumed to be frontal. Sakata and Teraki (2009) mentioned that it is theoretically very difficult to uniquely determine the rubble flow direction as a function of two horizontal components of ground motions, and so, they considered rubble flow direction probabilistically. For the present study, given that most buildings have openings in the front, and there are often structures on the other three sides which would help the structure to withstand collapse in those directions, it was assumed that the collapse would occur frontally, which is the worst possible direction with respect to road blockages.

Since we assumed that collapsed buildings would cause 3 m of blockage regardless of its height, we presumed that buildings that stand further than 3 m from the road would not cause road blockage even if they collapse.

5.3 Time required for evacuation

In our simulations, we estimated the number of successful evacuees by determining how soon after the evacuees would need to reach either the evacuation sites inside the area or the exit points to the external evacuation site, that is, Tokei Shrine. The reason why we need to set the exit points in the eastern side of the target district is as follows: In this simulation, we exclude the area between the eastern side of the target district and Tokei Shrine. Therefore, we first calculate the required time to go to Tokei Shrine from these points and estimated the time to get out of these points. When evacuating to Tokei

Shrine, we assumed that it would be 27 min after the earthquake before the tsunami reached the area surrounding the shrine and that the evacuee may take 14 min to reach to the shrine after getting out from the target district and additionally 2 min to climb up to the sufficiently elevated ground. Therefore, the evacuee must reach the exit point by 11 min after the earthquake. The time required to reach the shrine (14 min) was calculated based on the distance from the western end of the target district to the shrine, approximately 620 m, divided by 2.65 km/h, the average walking speed of residents older than 10 and younger than 70. In order to evacuate to buildings inside (the NTT building or the Primary School), we assumed that it would require 2 min to reach the roof of each building, so $t - 2$ is the time limit for evacuation, where t represents the time when the tsunami reaches the building, that is, 17 min for the NTT building and 19 min for the Primary School. The time limits for successful evacuation are summarized in Fig. 9.
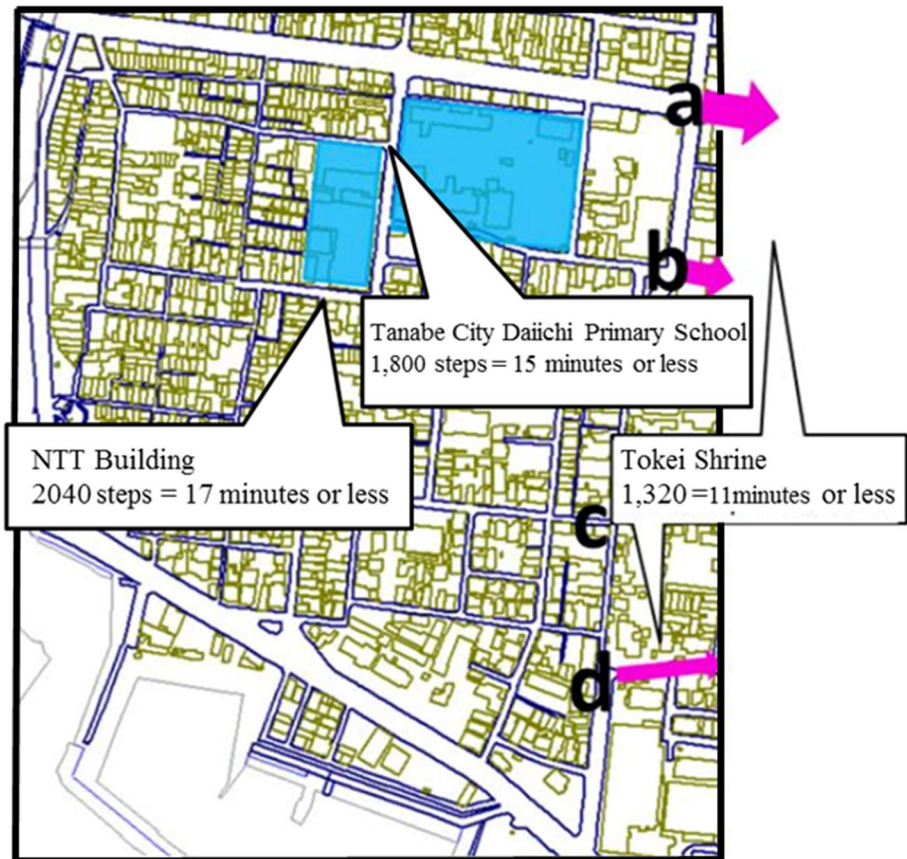

Fig. 9 Elapsed time from the beginning of the earthquake at each evacuation site for successful evacuation from the tsunami front. Four exit points on the eastern side of the target district, a–d, are defined for the outside evacuation site, Tokei Shrine

6 Tsunami evacuation simulation results and discussions

6.1 Evaluation of designated evacuation sites

First, the performance of the designated evacuation sites at present was evaluated under the assumption that there would be no building collapsed. By adding the evacuation buildings inside, namely the NTT building and the Primary School, 333 additional people, which is 27% of the whole residents, would be able to evacuate to these locations. However, 391 people, or 31.4% of the residents, would not be able to evacuate in time (Fig. 10). Thus, the current evacuation plan was found to be inadequate. It is necessary to consider additional evacuation sites in terms of numbers, locations, and their capacities to save all the residents in time. When we see the progress of evacuation in our simulation (Fig. 11), we found universal congestion around the three-storied RC building circled in red. Therefore, this building seems to be appropriate as an additional tsunami evacuation building to increase the number of successful evacuees.

6.2 Change in the number of successful evacuees as earthquake resistance reinforcement rates improve

By improving the proportion of earthquake-resistant houses from 0 to 100%, road blockages due to building collapse were eliminated. It was found that an additional 3% of residents could successfully evacuate for Case 1, or an additional 3.6% for Case 2 (Fig. 12). In this figure, the legends "Shrine a," "Shrine b," "Shrine c," and "Shrine d," respectively, refer to the group of residents who passed through the exit points a, b, c, and d to Tokei Shrine as shown in Fig. 9. The legends "School" and "NTT" refer to the residents that evacuated to these buildings. Please note that there was no one who passed the point "d" in Case 1. The aim here was to calculate the number of people originally who would take too much time to evacuate due to road blockages caused by collapsed houses and be caught by the tsunami despite having successfully escaped their homes, and would be saved thanks to measures to increase earthquake resistance of houses inside the target district.

 The study did not consider the number of people who may have died directly due to houses collapsing—either crushed to death or trapped until the tsunami arrived. With
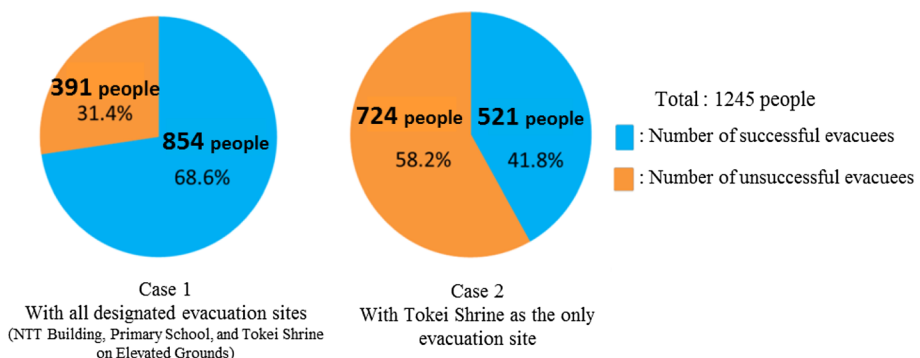

Fig. 10 Comparison of successful evacuation rate with (Case 1) and without (Case 2) the current evacuation sites inside the target district
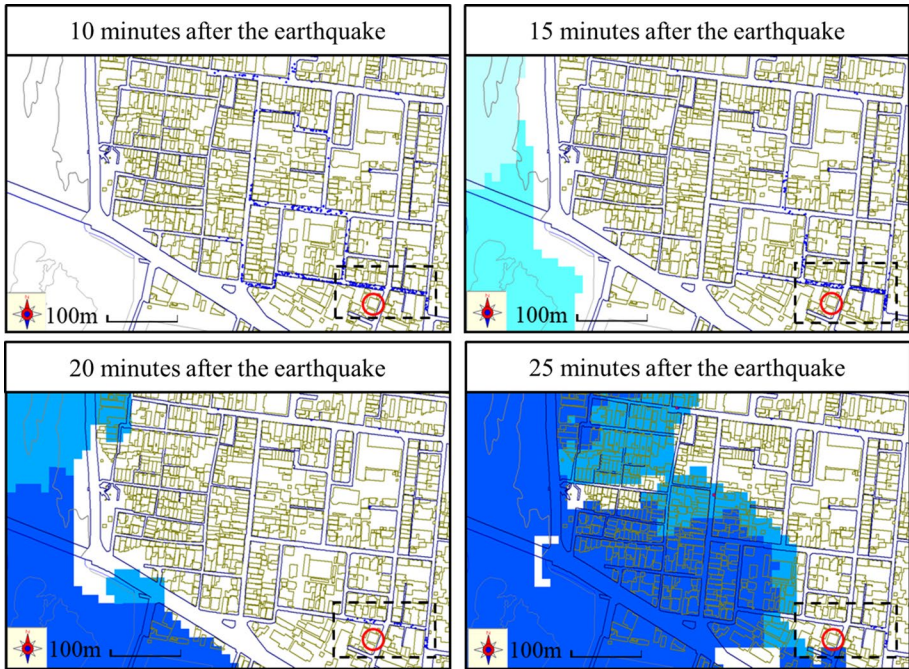
Fig. 11 Snapshots of the evacuation process for every 5 min from 10 min after the earthquake. Small dots on the streets represent evacuees. We definitively needed one or more evacuation sites in the southeastern side of the district, as shown by a rectangular with broken lines, in order to save evacuees in that area before the tsunami hit. A three-storied RC building circled in red can be a candidate for an additional evacuation site
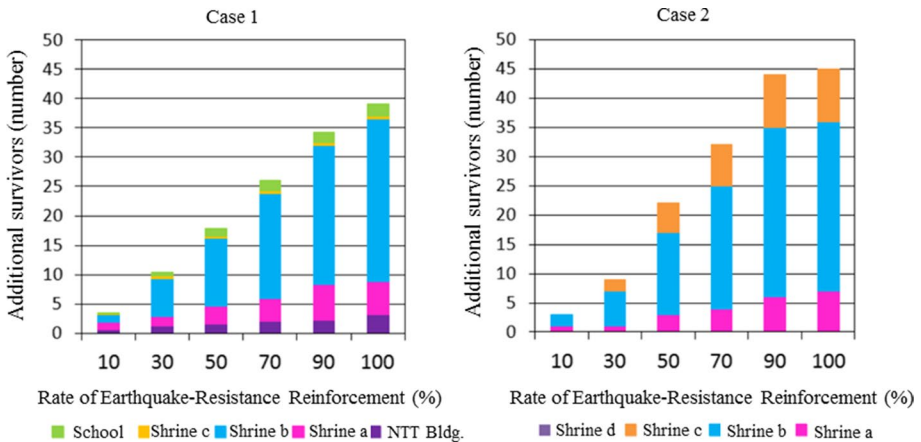

Fig. 12 Increase in the numbers of successful evacuees with increased earthquake-resistant reinforcement rates for Case 1 and Case 2. We can see that the additional survivors by the reinforcement would be 45 or 4% of the total evacuees at most

regard to this last point, the Central Disaster Prevention Council (2003) made the following estimate (Ministry of Construction, Building Research Institute 1996):

$$\begin{aligned} &\text{Numbers of fatalities due to collapsed wooden houses} \\ &= \text{numbers of totally collapsed wooden houses} \times 6.7\ \% \end{aligned} \tag{1}$$

$$\begin{aligned} &\text{Numbers of fatalities due to collapsed non-wooden houses} \\ &= \text{numbers of totally collapsed non-wooden houses} \times 6.7\ \% \\ &\times \text{correction factor } (0.0155/0.0629) \end{aligned} \tag{2}$$

Applying Eq. 1 to 257 houses that were identified to be of wooden construction, where the number of total collapsed houses is 257×0.74 (see Sect. 5.2), the total number of fatalities due to wooden building collapse would be $257 \times 0.74 \times 0.067 = 12$. The number of buildings that collapsed completely in the above formula was assumed to be equivalent to the number of heavily damaged or collapsed buildings here, based on the criteria defined and used by the Ministry of Construction's Building Research Institute (1996). Less than one fatality would be calculated from Eq. 2 for non-wooden houses. Please note that the effect of these immediate fatalities on the number of initial evacuees is negligibly small.

Based on the above, the fatality rate directly or indirectly caused by building collapse can be obtained by adding 12 (derived using Eq. 1) and the number of failed evacuees derived from the simulations. For Case 1, this would be $12 + 38 = 50$, which corresponds to 4% of the total population in the district. For Case 2, this would be $12 + 45 = 57$, or 4.6% of the population. If we also take into account collapsed buildings of unknown construction, the number of fatalities related to building collapse would be higher. Thus, fatalities would decrease if the number of earthquake-resistant buildings was improved. These figures, 3–4% by road blockage plus 1% by collapsed buildings, are not so large compared to the number of additional people that could be saved by increasing or improving the evacuation sites as noted in 6.1. Furthermore, Fig. 12 shows that the number of successful evacuees increases almost linearly with the increased rate of earthquake-resistant reinforcement. This is mainly due to the fact that the soil amplification factor is homogenous in this district, and wooden construction buildings are evenly distributed, causing the number of collapsed buildings to vary inversely with respect to the percentage of earthquake-resistant houses.

6.3 Change in the time required to complete the evacuation of 90% of the population by improving the earthquake resistance

In this section, we examine the delay in arrival at evacuation sites caused by building collapses and how improvement in the proportion of earthquake-resistant buildings might reduce the time required for evacuation, by investigating the average elapsed time after the earthquake until 90% of residents complete evacuation. The reason why 90% was chosen, rather than 100%, is because this is when the increase in the number of successful evacuees converges. This is because after 90% of residents complete evacuation, the remaining evacuees tend to be separated from each other inside the trapped areas, and so, the time interval to complete evacuation between one person and the next is getting larger and larger.

While we see some variation in the outcome depending on the evacuation sites, the time required for evacuation was reduced by approximately 30–60 s by improving the rate of earthquake-resistant houses from 0 to 100% (Fig. 13). Since residents must reach the evacuation site within 11 min after the onset of the earthquake if evacuating to Tokei Shrine, 15 min to the Primary School, and 17 min to the NTT Building for successful evacuation, the reduction in evacuation time of 30–60 s did not significantly increase the number of survivors as shown in Fig. 12. The influence of reinforcing buildings and houses on the number of successful evacuees is not so significant that increasing the capacity of evacuation sites looks more effective to reduce tsunami casualties. However, we did not consider any side effects of building damage on the speed of evacuation. If we have severe damage to the residential structure, first the start-up time of evacuation for residents will be increased because they need time to check the security of all the family members. Second, debris inside and outside of the damaged buildings will prevent smooth evacuation. Third, injuries to the residents inside the damaged buildings may cause further delay in their evacuation. If we combine these side effects into our simulation, the effects of building reinforcement would be more rewarding than the direct influence considered in this paper.

From the above results, it has been quantitatively determined that increasing the number of evacuation sites at appropriate locations is the highest priority. After having improved the numbers and locations of evacuation sites, increasing the percentage of houses with earthquake-resistant reinforcement would have a certain level of effectiveness as well.
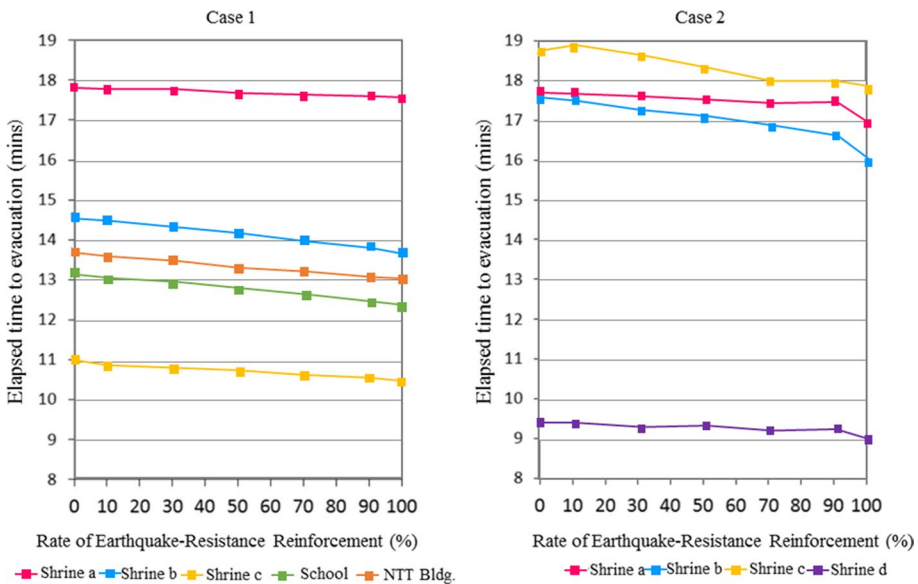

Fig. 13 Decrease in the elapsed times required for evacuation (for 90% of the total evacuees) with increased earthquake-resistant reinforcement rates for Case 1 and Case 2. We can see that the gain by the reinforcement would be around 60 s at most

7 Summary and future tasks

In this study, the building collapse ratio simulation program developed by Nagato and Kawase (2001, 2002a, b) was used to predict building collapses in the Tanabe City district in Wakayama Prefecture, where it is expected to have significant damage from both earthquake and tsunami during the earthquake scenario with the whole Tokai, Tonankai, and Nankai segments ruptured. Tsunami evacuation simulation was undertaken assuming road blockages from the predicted building collapses. We found that the prepared countermeasures are not enough to let everyone evacuate and that the number of survivors increases by 3–4% if all the houses were seismically reinforced. Considering this, plus only 1% of expected casualties inside the collapsed houses, it appears as though it is not as efficient to reinforce buildings and houses to prevent human loss in comparison with increasing the capacity of tsunami evacuation sites in the target district. However, the damage to building and houses will cause a lot of side effects which are not considered here, but must prolong the evacuation time. Thus, we concluded that we need to reinforce the houses as well as considering the appropriate placement, number, and capacity of the evacuation sites.

Even in the target district where relative consciousness toward disaster prevention is higher than in other districts, and evacuation planning is deemed more advanced, it was found that there are unresolved issues. As discussed in the building collapse prediction in this evacuation simulation, although fatalities from the collapsed buildings themselves and the effect of injuries on evacuation speed remained to be set as a parameter in the simulation, this study was able to quantify the risk of collapsed buildings in the evacuation process through the use of a building collapse ratio simulation program. This is a significant contribution to future studies and disaster prevention planning. We hope to continue to investigate evacuation predictions by extending the model that incorporates the direction of building collapse, variation in initiation time of evacuation, interaction between evacuees and cars and/or motorcycles, and fire breakout and subsequent spreading after the earthquake. We also hope to expand the size of the target district and perform more realistic simulations, thereby enhancing evacuation planning and residents' awareness.

References

Akakura Y, Takahashi H, Nakamoto T (2000) An attempt to model street blockage for prediction of earthquake damage in urban coastal area. Rep Port Harb Res Inst 39(4):19–41 **(in Japanese)**

Baoyintu (2014) Study regarding the quantitative damage estimation for a massive earthquake in southwest japan and countermeasures, Dissertation, Graduate School of Engineering, Kyoto University **(in Japanese)**

Baoyintu, Kawase H, Matsushima S (2013) Strong motion observed during the 2011 Great East Japan earthquake and its destructive powers, Architectural Institute of Japan. Papers from the Great East Japan earthquake 2nd anniversary symposium, pp 293–298 **(in Japanese)**

Central Disaster Prevention Council (2003) Disaster estimations for Tonankai–Nankai Earthquake and the summary of estimation methodologies. http://www.bousai.go.jp/kaigirep/chuobou/senmon/tounankai_nankaijishin/6/pdf/siryou3.pdf. Accessed 20 June 2018 **(in Japanese)**

Central Disaster Prevention Council (2011) Regarding Tokai, Tonankai, and Nankai Earthquakes. http://www.bousai.go.jp/jishin/nankai/model/1/pdf/2.pdf. Accessed 20 June 2018 **(in Japanese)**

Central Disaster Prevention Council (2012) Regarding Tokai, Tonankai, and Nankai Earthquakes (Second report). http://www.bousai.go.jp/jishin/nankai/model/pdf/20120829_2nd_report01.pdf. Accessed 20 June 2018 **(in Japanese)**

Geospatial Information Authority of Japan (2013) Maps and geospatial information. Webpage http://www.gsi.go.jp/kiban/index.html. Accessed 20 June 2018

Goto Y, Affan M, Agussabti NurdinY, Yuliana DK, Ardiansyah (2012) Tsunami evacuation simulation for disaster education and city planning. J Disaster Res 7(1):92–101

Hatayama M (1999) Development of space-time geographic information systems DiMSIS, GIS—theory and application, 7/2, pp 25–33 **(in Japanese)**

Ho N, Kawase H (2008) Damage prediction and earthquake risk management strategy for environmental load by the next Nankai earthquake. Compr J AIJ 6:87–92 **(in Japanese with English abstract)**

Hori M, Suematsu T, Araki H, Okumura Y, Dohi Y (2015) Verification and validation of tsunami evacuation simulation models. J Jpn As Earthq Eng 15(4):144–157 **(in Japanese with English abstract)**

Kamae K, Irikura K (1994) Strong ground motion evaluation in the near source and the surrounding area at the time of the 1946 Nankai earthquake (Mw=8.1). J Struct Constr Eng Trans AIJ 455:61–71 **(in Japanese with English abstract)**

Kaneda T (2010) Introduction to pedestrian agent simulation using Artisoc: from principle and methodology to space design and management for safety and crowd", Kozo Keikaku Engineering Inc., Shoseki Kobo Hayama Publishing **(in Japanese)**

Karim KR, Yamazaki F (2002) Correlation of JMA instrumental seismic intensity with strong motion parameters. Earthq Eng Struct Dyn 31:1191–1212. https://doi.org/10.1002/eqe.158

Kawase H (2007) Strong motion data of intensity seismometer (Shindo-kei) during the West off Fukuoka earthquake of 2005 and their structural damage potential. J Jpn As Earthq Eng 7(2):190–204 **(in Japanese with English abstract)**

Makinoshima F, Imamura F, Abe Y (2016) Behavior from tsunami recorded in the multimedia sources at Kesennuma City in the 2011 Tohoku tsunami and its simulation by using the evacuation model with pedestrian-car interaction. Coast Eng J Jpn Soc Civ Eng 58(4):1640023-1-28

Mas E, Suppasri A, Imamura F, Koshimura S (2012) Agent-based Simulation of the 2011 Great East Japan earthquake/tsunami evacuation: an integrated model of tsunami inundation and evacuation. J Nat Disaster Sci 34(1):41–57

Mas E, Suppasri A, Srivihok P, Koshimura S (2013) Feasibility of evacuation at the Pakarang Cape in Thailand based on tsunami inundation model and human evacuation simulation. In: 10th International conference on urban earthquake engineering, Tokyo, Japan, pp 1–6

Matsushima S, Kawase H (2000) Multiple asperity source model of the Hyogo-Ken Nanbu earthquake of 1995 and strong motion simulation in Kobe. J Struct Constr Eng Trans AIJ 534:33–40 **(in Japanese with English abstract)**

Ministry of Construction, Building Research Institute (1996) A survey report for building damages due to the 1995 Hyogo-ken Nanbu earthquake, BRI, Tsukuba

Ministry of Land, Infrastructure, Transport and Tourism (2012) City Department, Survey on the method for restructuring the cities suffered from the tsunami (Summary), MLIT, Tokyo **(in Japanese)**

Ministry of Land, Infrastructure, Transport and Tourism, City Bureau, Urban Transport Facilities Division, City Planning Division (2011) Great East Japan Earthquake tsunami damage field survey (Stage 3 Report)—field study of tsunami evacuation (bulletin), MLIT, Tokyo, p 6 **(in Japanese)**

Murao O (1999) Study on the vulnerability function based on the observed damage statistics in 1995 Hyogoken Nambu earthquake, Dissertation, the University of Tokyo. http://hdl.handle.net/2261/51136 **(in Japanese)**

Murao O, Yamazaki F (2002) Building Fragility Curves for the 1995 Hyogoken-Nanbu Earthquake based on CPIJ & AIJ's Survey Results with detailed Inventory. J Struct Constr Eng Trans AIJ 555:185–192 **(in Japanese with English abstract)**

Nagato K, Kawase H (2001) Damage evaluation models of reinforced concrete buildings based on the building damage statistics and simulated strong motions. J Struct Constr Eng Trans AIJ 554:31–37 **(in Japanese)**

Nagato K, Kawase H (2002a) A set of dynamic models of steel buildings for damage evaluation. J Struct Constr Eng Trans AIJ 559:101–106 **(in Japanese with English abstract)**

Nagato K and Kawase H (2002b) A set of wooden house models for damage evaluation based on observed damages statistics and non-linear response analysis and its application to strong motions of recent earthquakes. In: Japan earthquake engineering symposium, Japan Association for earthquake engineering, No. 11, vol 2, pp 1315–1320 **(in Japanese with English abstract)**

Nakai F, Hatayama M (2013a) Development of agent-based simulation system for tsunami evacuation estimation. Presentations of the Committee of infrastructure planning and management, vol 47, CD-ROM **(in Japanese)**

Nakai F, Hatayama M (2013b) Evaluation of evacuation plan through an analysis of evacuation behavior and resident coordination: a case study examining disaster risk communication in Kuroshio City, Kochi Prefecture. In: Presentations of the committee of infrastructure planning and management, vol 47, CD-ROM **(in Japanese)**

Nakai F, Hatayama M, Yamori K (2014) A study on evaluation for community based planning process of tsunami evacuation using agent based simulation. In: Information Processing Society of Japan, SIG Notes, No. 127, 2014.3, pp 1–9 **(in Japanese)**

National Research Institute for Earth Science and Disaster Resilience (2013) Japan seismic hazard information station. http://www.j-shis.bousai.go.jp/. Accessed 20 June 2018

Okada S, Takai N (2004) Damage index functions of wooden buildings and reinforced buildings for seismic risk Management. 13th world conference earthquake engineering, Vancouver, BC, August 1–6, 2004, Paper No. 727

Sakata T, Teraki A (2009) A study about simulations for road blockage considering directions of rubble flow. Proc Inst Soc Saf Sci 25:2009 **(in Japanese)**

Sato H, Murakami H, Shimada T, Kozuki Y, Kurata K, Otani H (2002) A study on the evacuation from tsunami considering building collapses by the earthquake. Coast Eng J Jpn Soc Civ Eng 49(2002):311–315 **(in Japanese)**

Southern California Earthquake Center (2018) Working group: Unified Structural Representation (USR). https://www.scec.org/research/usr/. Accessed 20 June 2018

Suzuki S, Furubayashi T, Okumura Y, Kawada Y (2011) Tokai, Tonankai, Nankai earthquake and tsunami simulation considering sliding near trench axis. In: Proceedings of the 30th symposium of the Japan Society for Natural Disaster Science No. 30, pp 65–66 **(in Japanese)**

Tamura T, Nishihata T, Moriya Y, Takimoto K, Miura F (2005) Application of evacuation simulation method during tsunami inundation considering road blockage. Coast Eng J Jpn Soc Civ Eng 52(2005):1286–1290 **(in Japanese)**

Tanabe City (2012) Resident basic register: population and households by Town, Tanabe City **(in Japanese)**

Tanabe City (2013a) Tanabe City statistics. http://www.city.tanabe.lg.jp/kikaku/toukei/. Accessed 20 June 2018

Tanabe City (2013b) Resident basic register: population by town and age (in 5 year-intervals), Tanabe City **(in Japanese)**

Tanabe City (2014) Tanabe City Tsunami Hazard Map. http://www.city.tanabe.lg.jp/bousai/files/tsunami_p04-p05_shinsuishin.pdf. Accessed 20 June 2018

Tanabe City (2016) Tanabe City earthquake resistant reinforcement promotion plan. http://www.city.tanabe.lg.jp/kenchiku/kenchiku/files/tanabesitaisinkaisyusokusinkeikaku.pdf. Accessed 20 June 2018

Usuzawa H, Imamura F, Shuto N (1997) Development of the method for evacuation numerical simulation for tsunami events. In: Annual meeting of the Tohoku Branch Technology Research conference, Japan Society of Civil Engineers, pp 430–431 **(in Japanese)**